

University of Copenhagen

Niels Bohr Institute

Center for Quantum Devices

Bachelor's Thesis

**Analyzing current-phase relation in
Josephson junctions on
superconductor-semiconductor
heterostructures**

Author:

Thor Blokker Rasmussen

Supervisor:

Charles Marcus

June, 2018

Acknowledgements

Firstly thank you Charles Marcus for letting me have the opportunity to work on my bachelor's project at the Center of Quantum devices and enjoy its great people and experimental facilities. I would also like to thank the 2DEG team for being friendly, welcoming and having great patience with me and taking the time to explain things to me in an understandable way. Lastly I would like to extend a special thanks to Antonio Fornieri and Fabrizio Nichele who helped me immensely throughout the project being my day to day advisors and helping me keep the project on track.

Abstract

This thesis contains the work I have done to extract and analyze current-phase relation (CPR) data of Josephson junctions in asymmetric superconducting quantum interference devices (SQUID), realized in hybrid InAs/Al heterostructures, hosting a two-dimensional electron gas (2DEG). The analysis is done by fitting the data with the analytical expression for the CPR of short S-2DEG-S Josephson junctions, in which the supercurrent is carried by Andreev bound states (ABS). From these fits I extract an average transmission of the junction and qualitatively try to understand the nature of this average. This is done by assessing the amount of ABSs with high or low transmission by comparison with a simultaneously taken tunneling spectroscopy measurement.

Contents

1	Introduction	2
1.1	Superconductors	2
1.1.1	Cooper pairs	2
1.1.2	The Meissner effect	3
1.2	Two Dimensional Electron-Gas	4
1.3	Andreev-Reflection, Bound States and N-S interface	5
1.4	Tunneling Spectroscopy	6
1.5	Josephson junctions and SQUID's	7
1.5.1	The Josephson Effect	7
1.5.2	The Fraunhofer Pattern	8
1.6	The SQUID Device	9
1.6.1	Measuring the current-phase relation in a SQUID	10
2	Measurements of the CPR of the Topological SQUID	10
2.0.1	The Heterostructure	10
2.1	The device	11
2.2	Data	12
2.2.1	Extracting and Fitting the CPR	13
2.2.2	Device with small junction width 150nm	13
2.2.3	Device with small junction width 120nm	14
2.2.4	Device with small junction width 80nm	15
3	Discussion	16
4	Conclusion	18

1 Introduction

1.1 Superconductors

Superconductivity is a phenomenon observed in many metals and even other more exotic materials below a specific (material dependent) critical temperature. It is characterised by zero electrical resistance and the expulsion of magnetic flux from the bulk of the superconductor. It was discovered by Heike Kamerlingh Onnes in 1911[1], and remains of interest today due to it's application in quantum devices.

1.1.1 Cooper pairs

A microscopic theory for conventional superconductors was formulated in 1957 by Bardeen, Cooper, Schrieffer (BCS)[1]. The explanation for the occurrence of superconductivity is due to the formation of Cooper pairs ($k \uparrow, -k \downarrow$), i.e. couples of electrons near the Fermi surface with opposite momentum (k) and spin ($\uparrow\downarrow$) paired by an attractive potential mediated by the electron-phonon coupling[6][1]. The phenomenological picture explaining this potential is that at low temperatures, the phonon vibrations slow down and the variations in the positively charged ion lattice of the metal caused by electron-phonon coupling has a slower relaxation time. When this is slow enough to create a trailing positive charge accumulation following a passing electron, the next electron will be attracted to this and therefore, in effect, be attracted to the other electron[1]. (See fig. 1).

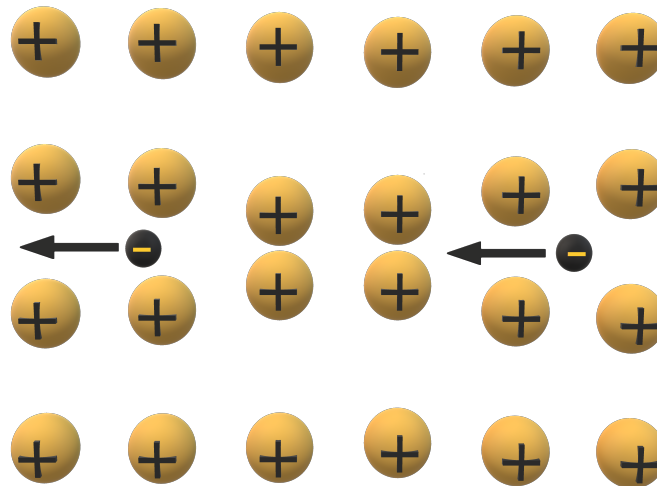


Figure 1: Picture showing the phenomenological picture of electron pairing mechanism forming Cooper pairs: the electron on the right sees an accumulation of the positively charged lattice ions caused by the passage of the electron on the left.

Thanks to this attractive interaction Cooper pairs behave as bosonic particles which condense into a single groundstate residing at the chemical potential (μ)[6]. The excited states of a superconducting system are fermionic quasiparticles ("Bogoliubov quasiparticles") con-

sisting of a linear combination of electron and hole-like states[6]. As shown in fig.2 an energy gap Δ_0 is opened around the chemical potential (μ) in the density of states owing to the attractive interaction between the electrons in the ground state. A Cooper pair has to absorb energy equal to $2\Delta_0$ to split up.

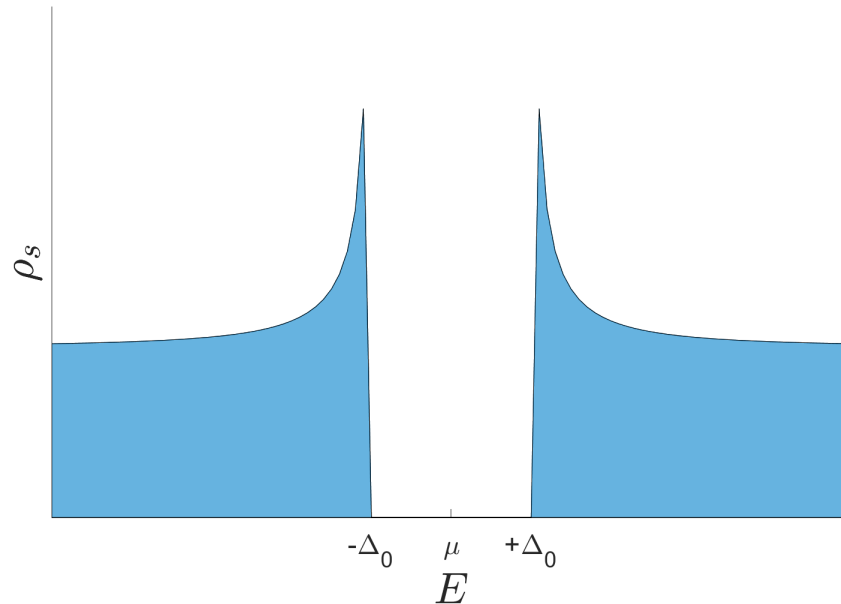


Figure 2: Plot showing the typical density of states (ρ_s) of quasiparticles in a superconductor with superconducting gap Δ_0 and chemical potential μ .

1.1.2 The Meissner effect

The Meissner effect is another special phenomenon connected to superconductors, where external magnetic fields are screened from the interior of the superconductor[1]. In other words, an external magnetic field (H) cannot penetrate the superconductor further than a certain penetration depth (λ). This effect was phenomenologically explained by the London brothers who obtained:[7]

$$\nabla^2 \mathbf{H} = \frac{1}{\lambda^2} \mathbf{H}. \quad (1)$$

This effect in addition to novel phenomena like levitating mercury it also leads to other effects such as critical magnetic fields for superconductors and flux focusing. The critical magnetic field stems from the fact that by screening an external magnetic field an internal one must be created by a current, to counteract the external one. This in turn costs energy and at a certain point it becomes energetically favorable to break the Cooper pairs with sufficient energy of $2\Delta_0$ [7]. Flux focusing is the name for the effective focusing of an external magnetic field. Imagine two superconducting blocks, infinite in all three spacial dimensions, but separated from each other by a small gap with either air or vacuum. A perpendicular magnetic field is applied, it gets expelled from the superconducting bulk and pushed into the gap between the superconductors, thus increasing the flux through this area.

1.2 Two Dimensional Electron-Gas

In condensed matter physics the notion of two-dimensional electron gases (2DEGs) is used to describe systems in which the motion of electrons is spatially confined in one of the three degrees of motion (the z direction, for instance) and free in the perpendicular plane (in the x and y directions). Thereby creating a two-dimensional system. One of the simplest ways of realizing a 2DEG is growing a series of layers of different semiconductors with different bandgaps. It is then possible to create a quantum well by "sandwiching" a small bandgap layer between two other layers with a larger bandgap[2][6]. (See fig. 3). This type of structure made up of different materials is also commonly referred to as heterostructures. Another special feature of such a two dimensional system is the fact that the density of states does not depend on the energy[8]:

$$\sum_n^N = \int_{-\infty}^{\infty} dn = \frac{L^d}{(2\pi)^d} \int_{-\infty}^{\infty} dk^d, \tag{2}$$

for 2d then:

$$\frac{L^2}{(2\pi)^2} \int_{-\infty}^{\infty} dk^2 = \frac{L^2}{(2\pi)^2} \int_{-\infty}^{\infty} 2\pi k dk, \tag{3}$$

and for parabolic dispersion with effective mass $E = \frac{\hbar^2 k^2}{2m^*}$, then by substitution:

$$\frac{L^2}{(2\pi)^2} \int_{-\infty}^{\infty} 2\pi \sqrt{\frac{2Em^*}{\hbar^2}} \sqrt{\frac{2m^*}{\hbar^2 E}} dE = L^2 \int_{-\infty}^{\infty} \frac{m^*}{2\pi\hbar^2} dE, \tag{4}$$

where $D_{2d}(E) = \frac{m^*}{2\pi\hbar^2}$ is the density of states for a 2DEG in periodic boundaries.

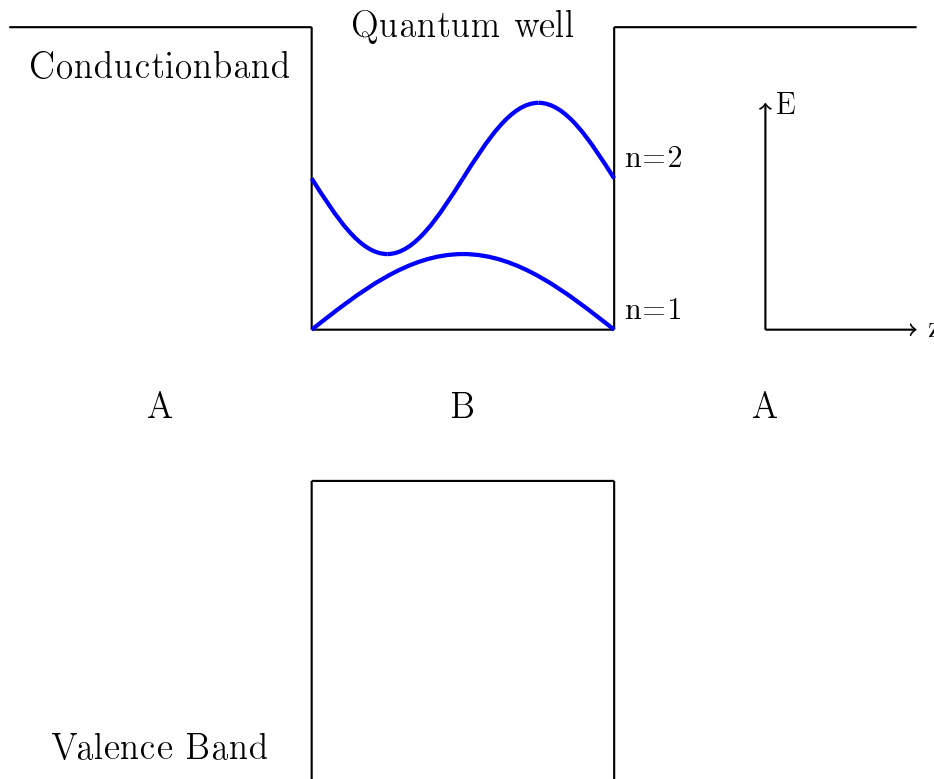


Figure 3: Simple illustration of band edge in a ABA heterostructure which forms a quantum well

1.3 Andreev-Reflection, Bound States and N-S interface

One of the fundamental features of a superconductor is its characteristic gap in the density of states as seen in fig.2. Now, consider a transparent interface between a normal metal and a superconductor(N-S interface). An electron coming from the normal side incident upon the N-S interface with energy above the chemical potential but below the gap, cannot be transmitted since there are no single electron states at that energy in superconductor. Additionally the absence of any barrier potential at the interface forbids normal reflection[6]. Now, the alternative is then called Andreev-reflection[6] a process in which a single electron couples to another electron from the Fermi sea of the normal metal and is transmitted as a Cooper pair through the N-S interface. Consequently, a hole is reflected back into the normal side. (See fig.4). This hole has the opposite spin and momentum of the incident electron since the Cooper pair must be formed from a pair of electrons with opposite spin and opposite momentum

($k \uparrow, -k \downarrow$). The rate between Andreev reflection and normal reflection depends on the interface transparency (the height of the barrier potential present at the interface)[6] which contributes to normal reflection, as shown in fig.5. The reflection probabilities shown in fig.5 comes from the Blonder-Tinkham-Klapwijk(BTK) model in which a delta function barrier is assumed at the interface[6]. The situation of Andreev reflection extends further when another superconductor is brought in contact with the normal metal to form an S-N-S junction. In this case, the hole reflected from first Andreev-reflection can again, because of time reversal symmetry, be Andreev-reflected from the second superconductor creating an electron that is identical to the one that was initially Andreev-reflected[6] (See fig.4). This mechanism forms a bound state reminiscent of the standing-wave modes in a Fabry-Perót interferometer, which effectively transfers Cooper pairs through the S-N-S junction. These Andreev bound states (ABS) are responsible for carrying the supercurrent in an S-N-S junction.

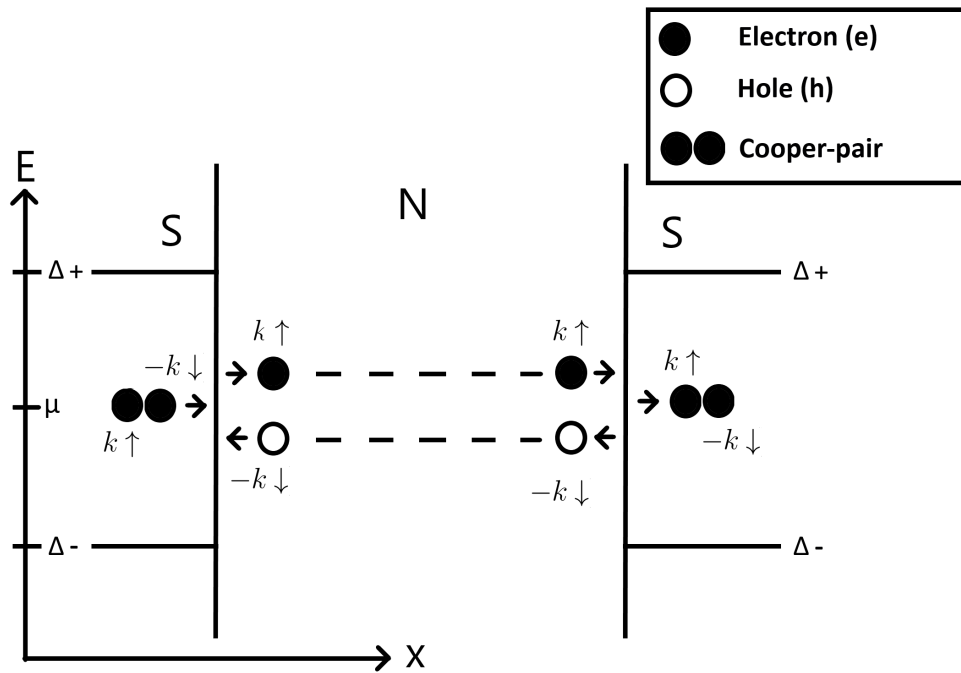


Figure 4: Schematic representation of the Andreev-reflection mechanism and Andreev bound states in an S-N-S

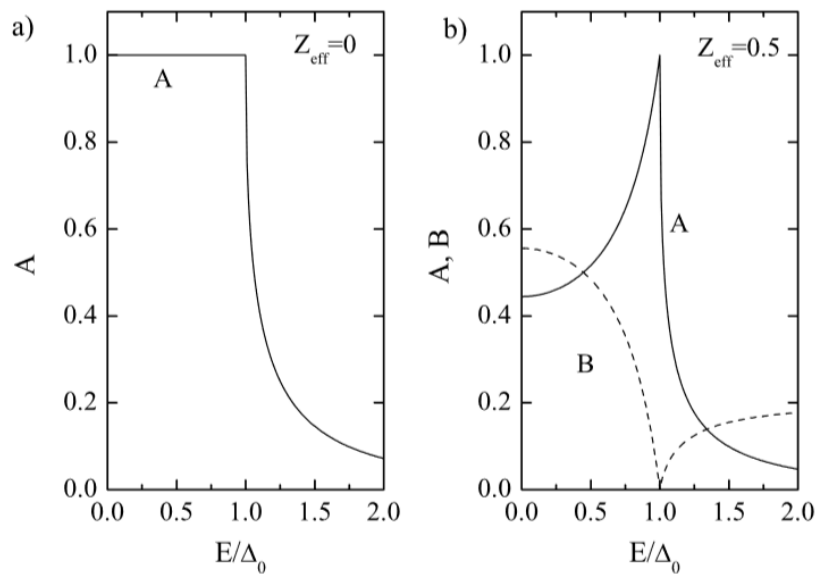


Figure 5: a) The Andreev reflection coefficient (A) as a function of $\frac{E}{\Delta_0}$ and for $Z_{eff} = 0$, where Δ_0 is the superconducting gap and Z_{eff} is the effective barrier transparency. b) The Andreev(A) reflection and the normal(B) reflection coefficients again as a function of $\frac{E}{\Delta_0}$ with $Z_{eff} = 0.5$. Figure from [6]

1.4 Tunneling Spectroscopy

Tunneling spectroscopy is used to probe the local density of states in a sample. This is done by connected the sample to an electron reservoir via a tunnel barrier so that transmission

can occur only through tunneling. The tunneling current between the two electron reservoirs is[2]:

$$I = -\frac{(2\pi)^2 |e|}{h} \int_{-\infty}^{\infty} \mathcal{T}(E) \mathcal{D}_R(E) \mathcal{D}_L(E) (f_L(E) - f_R(E)) dE \quad (5)$$

where $\mathcal{T}(E)$ is the tunneling transmission, $\mathcal{D}_{R/L}(E)$ is the density of states for the right and left reservoir and the $f_{L/R}$ are the Fermi distribution functions for the left and right reservoir. In the limit of temperature $T \rightarrow 0$, we can obtain:

$$\frac{dI}{dV_{SD}} = -\frac{(2\pi)^2 |e|}{h} \mathcal{T}(\mu_R + |e|V_{SD}) \mathcal{D}_R(\mu_R + |e|V_{SD}) \mathcal{D}_L(\mu_R + |e|V_{SD}) \quad (6)$$

If now both the tunneling transmission and the left reservoir density of states are independent of energy, the density of states of the right reservoir can be probed directly. These constraints turn out to often be satisfied when the probe is the apex of a metallic tip separated by a vacuum barrier to the conducting sample[2], or a normal metal in tunneling contact with the sample.

1.5 Josephson junctions and SQUID's

1.5.1 The Josephson Effect

In 1962 Josephson predicted that a zero voltage supercurrent (I_S) could flow between two superconducting leads (S) separated by an insulating barrier (I) (An S-I-S device).

$$I_S = I_C \sin(\Delta\phi) \quad (7)$$

Here $\Delta\phi$ is the phase difference between the Cooper pair condensate wavefunctions in the superconducting leads. This phase difference is connected to the voltage by:

$$\frac{d(\Delta\phi)}{dt} = \frac{2eV}{\hbar}. \quad (8)$$

Meaning that a constant voltage over the junction will linearly change the phase in time, generating an oscillating supercurrent. It turns out that the Josephson effect is more general and that any two superconducting leads separated by a non-superconducting "weak link" show this phenomenon. A weak link can be a normal metal (N) or a 2DEG. In the case of a semiconductor as a weak link, it is possible to control the local carrier density by applying an electrostatic potential with gates. In contrast to S-I-S Josephson junctions, in which the supercurrent is due to Cooper pair tunneling, the Josephson current in an S-N-S and S-2DEG-S junctions is carried by ABS. In the short junction limit, i.e., where the separation of the leads is much smaller than the superconducting coherence length, the current phase relation (CPR) may be described by[9]:

$$I(\phi) = \frac{e\Delta_0(T)}{2\hbar} \sum_{p=1}^N \frac{\tau_p \sin(\phi)}{(1 - \tau_p \sin^2(\frac{\phi}{2}))^{\frac{1}{2}}} \tanh \left(\frac{\Delta_0(T)}{2k_B T} \left(1 - \sin^2 \left(\frac{\phi}{2} \right) \right)^{\frac{1}{2}} \right), \quad (9)$$

where N is the number of ABS carrying the supercurrent through the Josephson junction and τ_p is the transmission of the p^{th} state.

From the eq.(9) we see that at low transmission the expression is near sinusoidal but at high transmission it is highly skewed (tending to a sawtooth like shape). These features of the CPR makes it useful for probing the transmission of the ABS carrying the supercurrent.

1.5.2 The Fraunhofer Pattern

The response of the critical current to a perpendicular magnetic field is equivalent to the Fraunhofer diffraction pattern in optics.

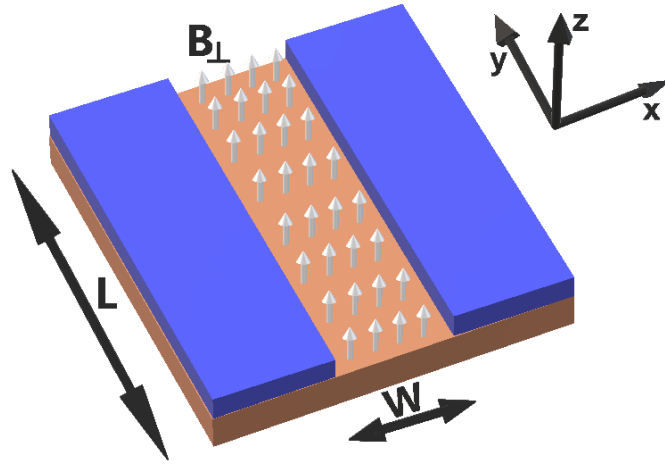


Figure 6: Schematic of the Josephson junction on 2DEG with perpendicular magnetic field penetrating the normal region with width (W) and length (L) contributing to a flux $\Phi = B_{\perp}WL$. The blue regions represent the superconducting leads which make the 2DEG underneath superconducting as well thanks to the proximity effect[7].

When considering the phase difference between the superconducting leads in the presence of a magnetic field (B_{\perp}) we have to consider the gauge-invariant phase:

$$\gamma = \Delta\phi - \left(\frac{2\pi}{\Phi_0}\right) \int \vec{A} \cdot d\vec{s}. \quad (10)$$

Here, \vec{A} the vector potential associated to the magnetic field, $\vec{B}_{\perp} = \vec{\nabla} \times \vec{A}$, and $\Phi_0 = \frac{h}{2e}$ is the superconducting flux quantum[7]. $\Delta\phi$ and γ can therefore also be used interchangeably when no magnetic field is present. Then for a rectangular junction the supercurrent density is

$$J_s = J_c \sin \left(\Delta\phi - \left(\frac{2\pi}{\Phi_0}\right) \int \vec{A} \cdot d\vec{s} \right) \quad (11)$$

In eq.(11) the integral is just the total flux inclosed by the junction (Stokes theorem) since the magnetic field decays exponentially into the superconducting leads. This results in a linear phase dependence[5][8]:

$$\frac{\partial\phi}{\partial y} = \frac{2\pi}{\Phi_0} B_{\perp} W \quad (12)$$

By combining (7) and (12) we obtain the following expression for the supercurrent[5]:

$$I_s(B_{\perp}) = \int_{\frac{L}{2}}^{-\frac{L}{2}} J_C \sin(ky + \phi_0) dy = \Im \left(e^{i\phi_0} \int_{\infty}^{\infty} J_C(y) e^{iky} dy \right) \quad (13)$$

with $k = \frac{2\pi}{\Phi_0} B_{\perp} W$. The maximum ("critical") Josephson current therefore reads[5]:

$$I_s^m(B_{\perp}) = \left| \int_{\infty}^{\infty} J_C(y) e^{iky} dy \right| = I_C \left| \frac{\sin(\frac{kL}{2})}{\frac{kL}{2}} \right| = I_C \left| \frac{\sin(\frac{\frac{2\pi}{\Phi_0} B_{\perp} WL}{2})}{\frac{\frac{2\pi}{\Phi_0} B_{\perp} WL}{2}} \right| = I_C \left| \frac{\sin(\frac{\pi\Phi}{\Phi_0})}{\frac{\pi\Phi}{\Phi_0}} \right|. \quad (14)$$

We see that the critical current is modulated by a Fraunhofer pattern identical to the one describing diffraction of light through a rectangular slit.

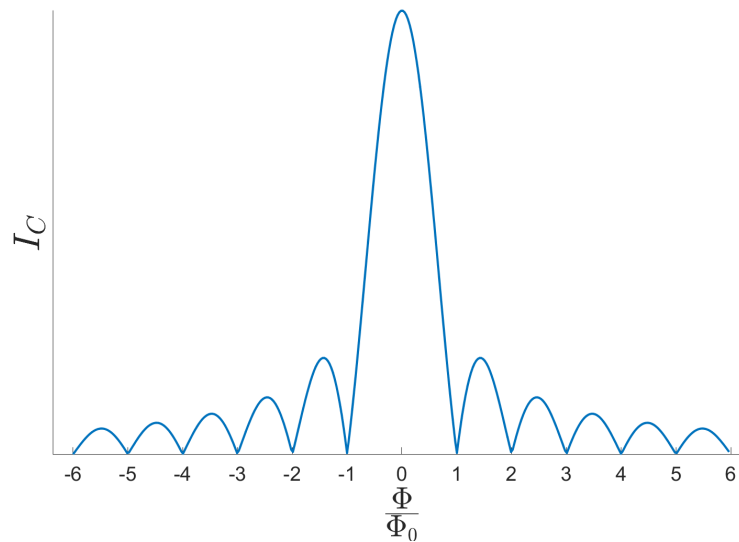


Figure 7: Plot of the fraunhofer pattern as in eq.(14)

1.6 The SQUID Device

The Superconducting Quantum Interference Device (SQUID) is a device consisting of two parallel Josephson junctions inserted into a superconducting ring and the prominent feature of such a device is the high sensitivity to small magnetic fields compared to a single Josephson junction. This is due to the increased flux area formed by the ring. Since the ring is superconducting the flux is still quantized as in the case of the Fraunhofer pattern. The supercurrent flowing through the SQUID is the sum of the two Josephson currents flowing through the junctions. In the case of a sinusoidal CPR as in eq.(7), we obtain[7]:

$$I_S = I_{c1} \sin(\phi_1) + I_{c2} \sin(\phi_2). \quad (15)$$

Now as in the case of Fraunhofer diffraction the gauge-invariant phase leads to a connection between phase and magnetic flux, in particular[7]:

$$\phi_2 - \phi_1 = \frac{2\pi\Phi}{\Phi_0}, \quad (16)$$

if the junctions have identical critical current i.e. the junction is symmetric, then by trigonometry we obtain the maximum supercurrent:

$$I_m = 2I_c \left| \cos\left(\frac{2\pi\Phi}{\Phi_0}\right) \right|. \quad (17)$$

1.6.1 Measuring the current-phase relation in a SQUID

In order to experimentally obtain the CPR of a junction it is possible to measure the $I_c(\Phi)$ of a SQUID with a reference junction characterized by a known CPR to then be able to separate the CPR of the junction of interest, with unknown CPR, from the $I_c(\Phi)$ data. Another way of measuring the CPR of a junction without a known reference is to fabricate an asymmetric SQUID such that the critical current of the junction of interest (I_{c2}) is much smaller than the critical current of the reference junction (I_{c1}). Then if, in eq.15 $I_{c1} \gg I_{c2}$ the phase difference of junction 1 is very close to $\pi/2$ [3] and is therefore approximately constant, while the phase of junction 2 varies from 0 to 2π if the flux is varied from 0 to Φ_0 . This method of utilizing an asymmetric SQUID device for measuring the CPR is the one used later in this work. The data analyzed satisfies the requirement $I_{c1} > 10I_{c2}$.

2 Measurements of the CPR of the Topological SQUID

The CPRs measured and shown are CPRs of a SQUID device similar to the one predicted by Pientka and collaborators [4] to detect a topological phase transition in parallel field. It is therefore interesting to characterize this kind of device by extracting the transmission probability of the ABSs from the skewness of the CPRs.

2.0.1 The Heterostructure

The devices are fabricated on wafers with heterostructure as shown in fig.8, grown by molecular beam epitaxy to make the interfaces as good as possible.

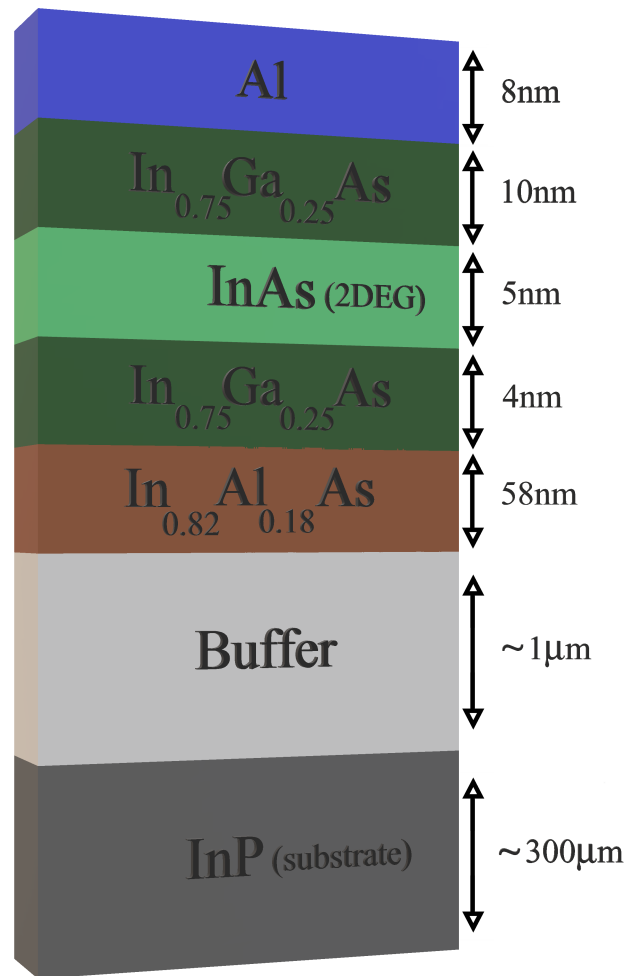


Figure 8: Schematic of the type of heterostructure used to define the 2DEG used in the devices

2.1 The device

Fig.9 shows the schematic representation of the measured devices. The Josephson junction of interest (called "top junction") is inserted in an asymmetric SQUID with a reference junction characterized by a larger critical current. The superconducting loop is defined by etching the 2DEG mesa (represented in light grey) and the epitaxial aluminum layer (blue) on top of that. In order to control the density in the 2DEG, top gates (yellow) are evaporated on top of the structure and they are isolated from 2DEG by 15 nm of insulating HfO_2 . The superconducting lead and the quantum point contact at the top are used to perform tunneling spectroscopy on the top junction. The reference junction is 40nm wide and 5μm long, the area of the SQUIDs are shown in table1. The length of of the top junction is always 1.6μm.

Table 1: Area of the SQUID loops extracted from the periodicity of the CPR

Device (By top junction width)	SQUID Area
120nm	15.45 μm^2
150nm	27.65 μm^2
80nm	25.52 μm^2

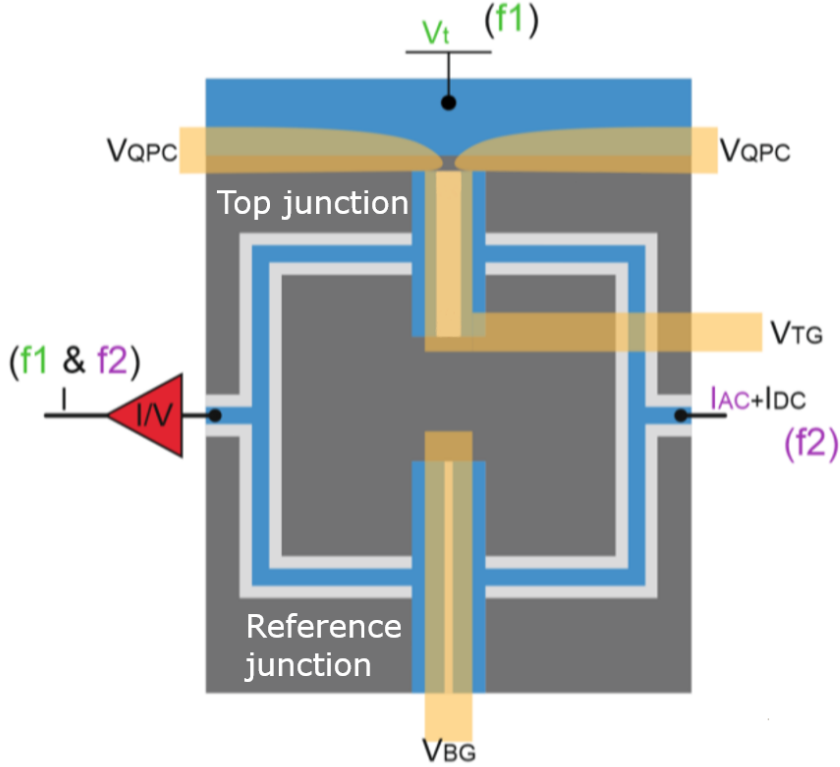


Figure 9: Schematic of the device type. Blue represents Aluminum, light grey represents the mesa (2DEG), dark grey indicates the non-conducting etched regions (etched down til the buffer layers of heterostructure stack see fig.8) and yellow represents the gates on top. V_t is the AC bias voltage at frequency f_1 that we apply to perform spectroscopy (through the QPC), while I_{ac} and I_{dc} are the AC and DC component of the current we are injecting at frequency f_2 to measure the Josephson critical current of the SQUID.

2.2 Data

The data presented in this thesis is set of CPR data, measured in several similar devices but with different widths of the top(small) josephson junction i.e. the one of interest. All data here are taken at 0 parallel magnetic field, although the devices were designed to be operated at high parallel magnetic fields to achieve the topological phase transition predicted by Falko Pientka et. al.[4]. The data is taken at 0 parallel field because these yield stable data to characterize the average transimission of the ABS in the Josephson junction, which is a parameter of interest for better understanding more advanced phenomena happening in the device.

2.2.1 Extracting and Fitting the CPR

To extract the CPR we measure the SQUID critical current as a function of magnetic flux. To do so we inject a dc-current through the SQUID and measure its differential resistance. The critical current is identified by the switch in the SQUID differential resistance when we sweep the dc-current I_{dc} . In the limit of $I_{c1} \gg I_{c2}$ the oscillations of $I_c^{SQUID}(\Phi)$ reflect the CPR of the top(small) junction of the SQUID[3]. Example of this raw data is shown in fig.10

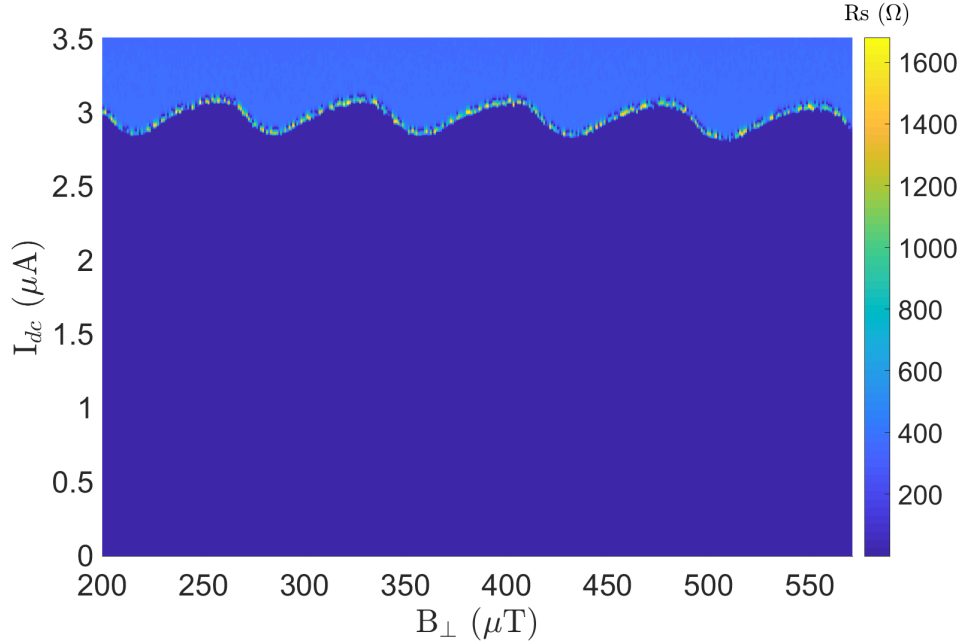


Figure 10: Plot of the raw data from which CPR is extracted. It is a 2d colormap of differential resistance versus dc-current and perpendicular magnetic field.

The field axis is then converted into normalized flux by using the geometry of the individual device, after which the data is fitted to eq.(9). From spectroscopy measurements we know that we have many ABS carrying the supercurrent. For simplicity we decide to fit the CPR with the short junction formula eq.9 accounting for just one Andreev bound state in order to extract the effective average transmission of the ABS in the junction. Another obstacle to extracting the correct CPR is the Fraunhofer-pattern since the actual raw data contains both the Fraunhofer-patterns and the CPR of both junctions. By calculating Fourier transform and squelching the lowest harmonics, we can isolate the CPR oscillations. This should always be possible as long as the area of the SQUID is significantly larger than that of both Josephson junctions.

2.2.2 Device with small junction width 150nm

The fit in fig.11 gives an average transmission of $\tau = 0.70$

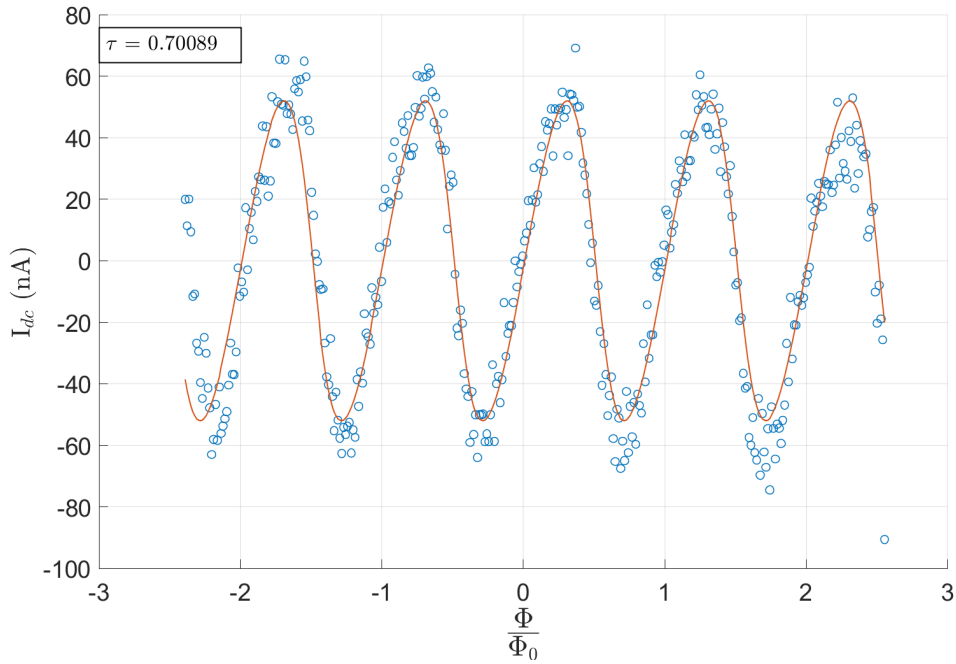


Figure 11: Plot of junction with width of 150nm after processed by Fourier transform to remove the Fraunhofer pattern background and fitted to eq.(9)

2.2.3 Device with small junction width 120nm

In this device we took two sets of CPR at different regimes of top gate voltage. First regime of $V_{TG} = -7mV$ the fit yields an average transmission of $\tau = 0.71$, for the second regime(fig.13) where $V_{TG} = -27mV$ the average transmission from the fit is $\tau = 0.64$.

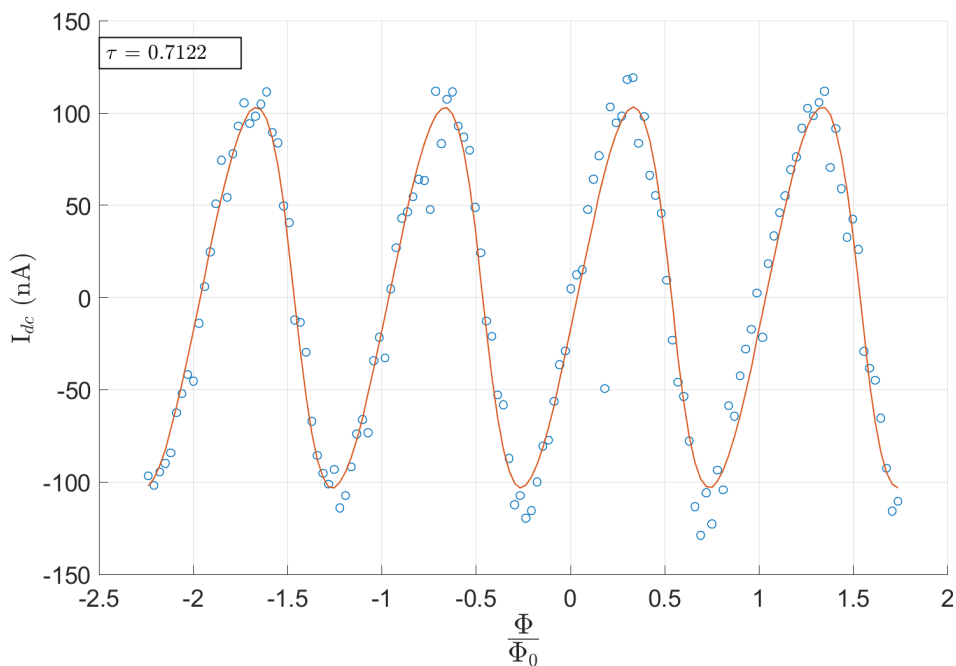


Figure 12: Plot of junction with width of 120nm after processed by Fourier transform to remove the Fraunhofer pattern background and fitted to eq.(9) in the first regime of $V_{TG} = -7mV$

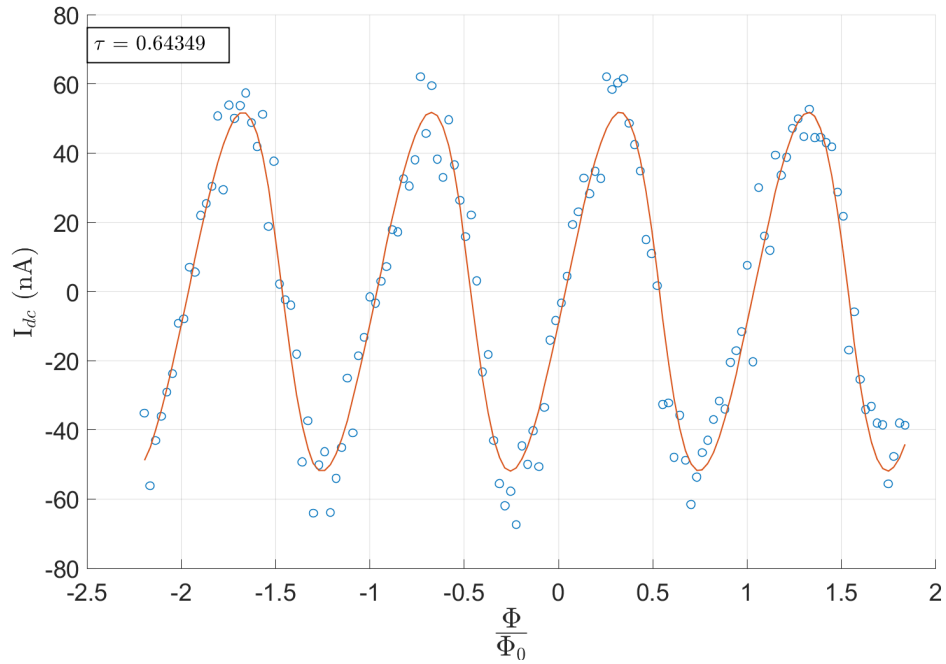


Figure 13: Plot of junction with width of 120nm after processed by Fourier transform to remove the Fraunhofer pattern background and fitted to eq.(9) in the first regime of $V_{TG} = -27mV$

2.2.4 Device with small junction width 80nm

The fit to the CPR of this device shows more highly skewed CPR and likewise high transmission of $\tau = 0.86$

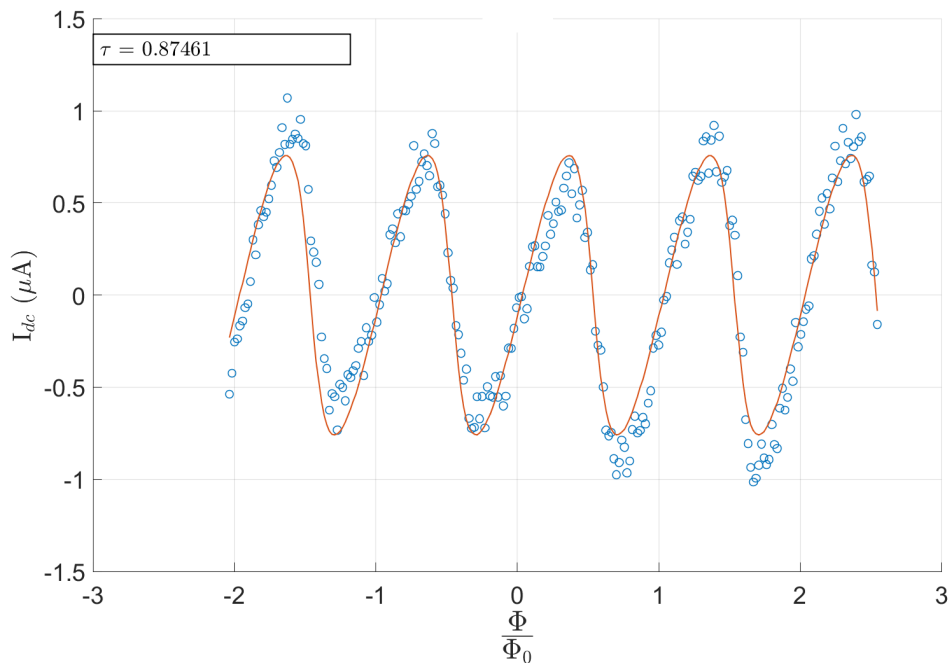


Figure 14: Plot of junction with width of 80nm after processed by Fourier transform to remove the Fraunhofer pattern background and fitted to eq.(9)

3 Discussion

The fits of the CPRs to only one mode of eq.(9) seems to qualitatively give a good transmission for the devices. However some flaws of this method of analysis quickly comes to mind, for instance: the fact that the information yielded from the fit is an average of the transmission of all the ABSs that contribute to the CPR and therefore gives no information about the individual ABSs, and that the nature of this average only lends this information to a qualitative understanding of the transmission. Information about the single Andreev bound state modes is therefore not possible with this method. Additionally CPR data was measured for a device with small junction width of 160nm , but it did not satisfy the requirement that $I_{c1} > 10I_{c2}$. Indeed, for the for the critical current of the 160nm wide junction the ratio between the amplitude of the oscillation (I_{c2}) and the background (I_{c1}) (See fig.15) is about 3.7.

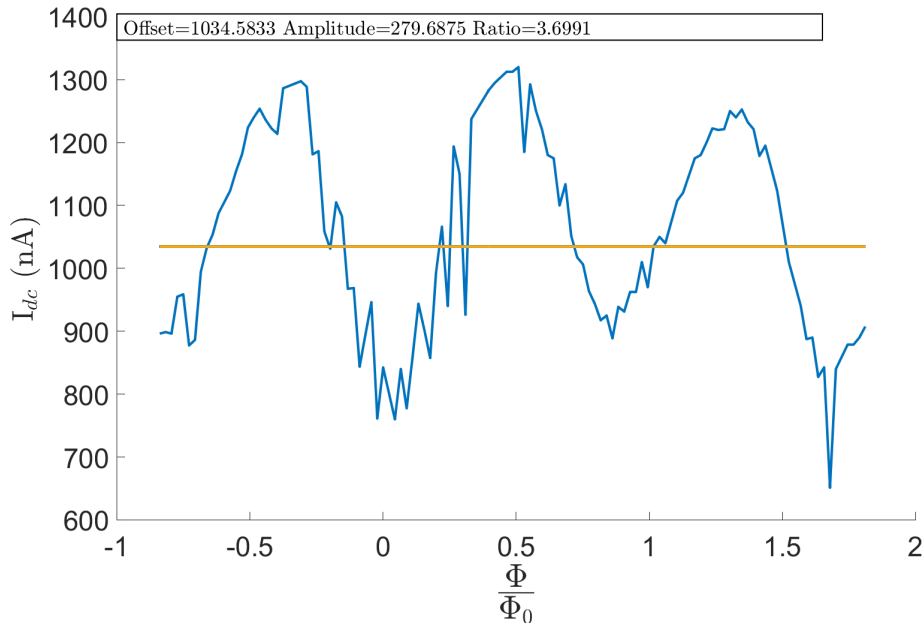


Figure 15: Plot of the extracted CPR data before fourier transform from the device with small junction width of 160nm zoomed in on the highest peaks to try and estimate the ratio of the amplitude of the CPR versus the constant offset which is used to determine the validity of the claim $I_{c1} \gg I_{c2}$

An average transmission in the range $0.64 - 0.86$ confirms the high quality of the Josephson junctions fabricated in the material. Regarding the fits, the short-junction formula eq.(9) seemed quite numerically unstable which further solidifies the use of them as mainly qualitative in nature. For this reason further statistical error analysis was not pursued. While fitting, especially for Fig.12 and Fig.13, the periodicity was off by a factor of about 1.2 which suggest flux focusing due to the Meissner effect or that the fabricated area differs from the schematic, which then effectively increases the flux area. This was not as big of an issue with the fit of Fig.11, where no correction was needed. The data from the 120nm junction device was taken simultaneously to tunneling spectroscopy measurements in an attempt to be able to compare these.

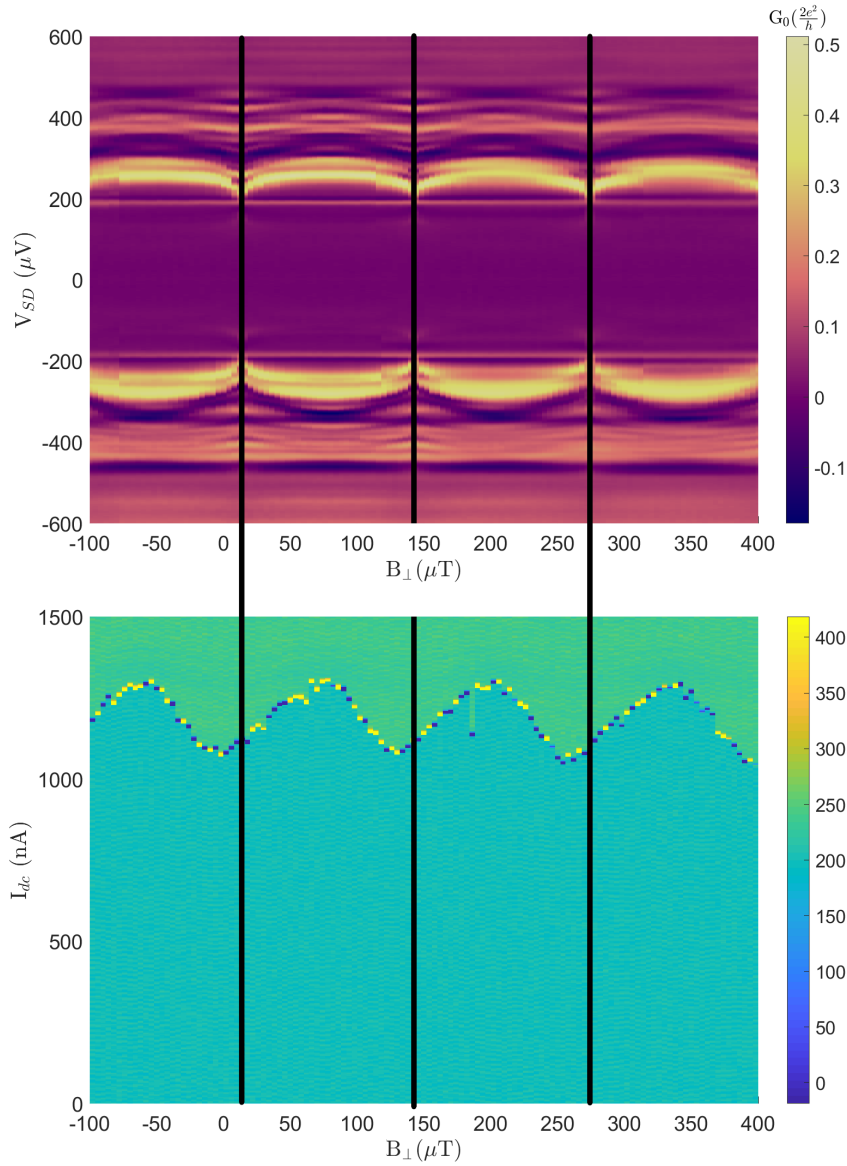


Figure 16: Plot of the extracted CPR data before and the spectroscopy data taken simultaneously with lines drawn to make the correlation of the two figures more clear. The spectroscopy is differential conductance in units of the quantum of conduction G_0 as a function of source-drain voltage and perpendicular magnetic field. From this we qualitatively observe what looks like 1 or 2 highly transmitting modes (the bright curves) and above these are many more faint structures which still seem to maintain periodicity and these would be lower transmission modes

In order to gain more information about the ABSs that carry the current, the comparison with the spectroscopy data taken simultaneous with the CPR was discussed (see fig.16). The ABSs in a Josephson junction depend on the phase difference between the leads as[10]:

$$E_{ABS,i} = \pm \Delta \sqrt{1 - \tau_i \sin^2 \left(\frac{\phi}{2} \right)}, \quad (18)$$

where Δ is the superconducting gap, ϕ is the phase difference between the superconducting leads and τ_i is the transmission of the i^{th} ABS. From eq.(18) it is evident that the energy of the ABSs do not go to zero at $\tau_i < 1$, in particular the oscillations of the ABSs energy in

phase has a constant maximum of Δ , but the amplitude diminishes with lower transmission τ_i . Then from eq.(18), qualitatively it seems that the ABS curves in the spectroscopy (fig.16) that line up in periodicity with the CPR tend to indicate that we have few highly transmitting modes and many low transmitting modes which then could, again qualitatively, reasonably make up the average transmission in the range 0.64 – 0.86. Now the picture in fig.16 is complicated by the fact that also the tunneling probe is superconducting and characterized by a gap $\Delta_{lead} \simeq 200\mu eV$. The measure of differential conductance is therefore the convolution of two superconducting densities of states. The most transparent ABSs in the junction are therefore modulated between $\Delta_{lead} + \Delta_{junction} \simeq 300\mu eV$ and $\Delta_{lead} \simeq 200\mu eV$.

4 Conclusion

In conclusion I have analyzed the current-phase relation of of superconductor/semiconductor Josephson junctions inserted in asymmetric SQUIDs. This kind of structures are predicted to be a promising candidate for the study of topological superconductivity[4] In this work, we limited the study to the CPRs and to the extraction of the transmission in order to characterize the quality of the Josephson junctions of the SQUID. I find on different devices similar transmission in the range 0.64 – 0.86 which corresponds to quite transparent S-2DEG-S. Another qualitative observation was that by comparing simultaneous spectroscopy and CPR measurements it seemed reasonable that the average transmission consisted of few highly transmitting ABS modes and many low transmission ones.

References

- [1] Stephen Blundell *"Superconductivity: A Very Short Introduction"*, ISBN: 978-0-19-954090-7
- [2] Thomas Ihn (2010) *"Semiconductor Nanostructures: Quantum States and Electronic Transport"*, pp. 198-199 and ch. 5 ISBN: 978-0-19-953443-2
- [3] Gaurav Nanda, Juan Luis Aguilera-Servin, Péter Rakyta, Andor Kormányos, Reinhold Kleiner, Dieter Koelle, Kenji Watanabe, Takashi Taniguchi, Lieven M. K. Vandersypen, Srijit Goswami: *"Current-phase relation of ballistic graphene Josephson junctions"*, arXiv:1612.06895 (2016)
- [4] Falko Pientka et. al. *"Topological Superconductivity in a Planar Josephson Junction"*, arXiv:arXiv:1609.09482 (2016)
- [5] Prof. Gross and Dr. Marx *Lecture Notes on "Applied Superconductivity"*, Chapters 2 & 4, URL:
https://www.wmi.badw.de/teaching/Lecturenotes/AS/AS_Chapter2.pdf,
https://www.wmi.badw.de/teaching/Lecturenotes/AS/AS_Chapter4.pdf
- [6] Thomas Schäpers (2001) *"Superconductor/ Semiconductor Junctions"*, ISBN: 3-540-42220-X
- [7] Michael Tinkham (1996) *"Introduction to Superconductivity"*, ISBN: 0-07-064878-6
- [8] Henri J. Suominen PhD thesis (2017) *"Two-dimensional Semiconductor-Superconductor Hybrids"*,
- [9] Eric M. Spanton, Mingtang Deng, Saulius Vaitiekėnas, Peter Krogstrup, Jesper Nygård, Charles M. Marcus, and Kathryn A. Moler: *"Current-phase relations of few-mode InAs nanowire Josephson junctions"*, Nature Physics volume 13, pp.1177–1181 (2017)
DOI:10.1038/NPHYS4224
- [10] David J. van Woerkom, Alex Proutski, Bernard van Heck, Daniël Bouman, Jukka I. Väyrynen, Leonid I. Glazman, Peter Krogstrup, Jesper Nygård, Leo P. Kouwenhoven, Attila Geresdi: *"Microwave spectroscopy of spinful Andreev bound states in ballistic semiconductor Josephson junctions"*, Nature Physics volume 13, p.876 (2017)
DOI:10.1038/nphys4150